

DESIGN OF FIELD ORIENTED CONTROL USING IMPROVED FLUX CONTROLLER FOR PERMANENT MAGNET SYNCHRONOUS MOTOR IN TRACTION DRIVE

CHITRA VENUGOPAL

Utilities Engineering, The University of Trinidad and Tobago, Point Lisas Campus, Trinidad
E-mail: chitra.venugopal@utt.edu.tt

Abstract

In traction applications, PMSMs are gaining attention due its reliability and wide constant power speed ranges. The high maintenance cost and complicated control methods are the disadvantages of PMSM. The efficiency of PMSM can be increased to suit the requirements of traction applications by achieving direct control of stator current. However it is quite unattainable due to the strong coupling and non-linear nature of PMSM. To decouple the motor variables, field oriented control technique is commonly used. In this paper, the closed loop control of PMSM using improved flux weakening controller is designed and simulated using Matlab/Simulink. The performance of the motor is tested under running mode operation with load. The simulation results shows good dynamic response of the drive with less ripples for varying speed and load torque. Also, RLC filter is designed to reduce the voltage and current harmonics at motor terminals. The improved flux weakening control method regulates the magnetic flux throughout the entire speed profile. This can be seen from the results that the desired speed is achieved with 2.6% of ripple for mechanical load torque ranging from 200 Nm to 800 Nm whereas the reference speed is maintained at 500 rad/s. Also, it can be seen from the results that the controller adjusts the stator current component automatically without causing spikes during switching and hence the PMSM motor can be driven without setting the direct component of stator current to zero and DC bus voltage is maintained constant at 560 V.

Keywords: PMSM, Traction drive, Field oriented control, Flux weakening controller, PI controller, DC-DC fly back converter, Voltage source Inverter.

Nomenclatures

Abbreviations

AC	Alternating Current
DC	Direct Current
FOC	Field Oriented Control
IGBT	Isolated Gate Bipolar Transistor
MTPA	Maximum Torque Per Ampere
PI	Proportional Integral Controller
PMSM	Permanent Magnet Synchronous Motor
PWM	Pulse Width Modulation
THD	Total Harmonic Distortion
VSI	Voltage Source Inverter

1. Introduction

A traction system is an integrated system of power converters, traction motors, protection and regulation circuits intended to generate tractive forces to provide relative motion in different applications. These systems are widely used in electric vehicles, mining and railway locomotives.

Traditionally, DC motor drives have been used in traction drives due to low cost of implementation and ease of control. The drawbacks of DC motors in traction applications are low overload capacity, lower torque than AC motors and higher maintenance on brushes and commutate. These drawbacks have made AC motors to replace DC motors in industrial applications [1].

The requirements of the traction drive system have been best suited for Permanent Magnet Synchronous Motor (PMSM) and hence it is considered as the most promising motor in tracking applications due its advantages compared to induction and DC motors [2].

These advantages attract PMSM in traction drive applications for replacing induction motors and DC motors. However PMSM has some drawbacks such as high maintenance cost and magnets heat up which are commonly related to the permanent magnets and control methods.

In order to achieve the desired and effective performance of PMSM in traction applications, direct control of stator currents is required. However it is quite unattainable due to the strong coupling and non-linear nature of PMSM. To decouple the motor variables field oriented vector control method must be used to achieve faster dynamic response at different modes of operation.

To achieve this different methods has been proposed. In the field oriented control inserting a decoupling block in between the PI controller and PWM controller is tested in [3]. It is proved to improve the performance of PMSM in running mode. However the actual current over the set point can be observed.

Zhang [4] discussed the effects of setting the direct component of stator current to zero throughout the speed range. The effects include high currents in stator winding resulting in more losses. In order to minimize the losses, MTPA is proposed as the best solution [5]. Though this method proves to be an efficient

method, according to the discussion presented in [6] this method is most suitable for interior permanent magnet motors due to saliency property.

To overcome the disadvantages of the above method, flux weakening control is proposed in [7]. The speed range is widened in this method whereas the current spikes are observed to be high in this method. To avoid the current spikes, functional model predictive control method is employed in [8] which involves huge computations.

In general, the flux weakening method commonly suffers from limited constant power- speed ratio, current control instability and low torque control. Another challenge in using flux weakening method is operating the motor at constant power region.

In order to overcome the drawbacks of flux weakening controller, feedback method is proposed in [9]. The feedback method is affected by the high integrator gain which creates oscillations around torque set points and magnitude overshoots. The direct drive system for PMSM in railway application is proposed in [10]. The direct drive system reduces the control complexity whereas the noise and temperature rise has become unavoidable.

The prediction of torque component method to control the speed of PMSM is proposed in [11]. This method proved to overcome the drawbacks of feedback method, however the inaccuracy in the prediction method limits the inverter output voltage.

Also, the traction systems require different voltage levels and power converters play the role of transformer for efficiently transforming the desired DC voltages in these traction systems. A bi-directional multi input DC-DC converter topology capable of boost during motoring mode and buck mode during braking mode to charge a battery system is presented in [12]. Although the converter provided more power to the system, it had drawbacks of power losses due to switching and conduction. Also the bi-directional flow of power requires effective protection and regulation systems that monitor the flow.

A boost integrated fly-back converter is proposed in [13]. It has achieved a high level of performance by forcing each energy storage element to change its state as independent as possible. The major disadvantage of this topology is excessive voltage across the output capacitor under different load conditions. Jil et al.[14] stated different solutions for this problem which include the simultaneous phase shift and duty ratio control to independently regulate the output voltage across the output capacitor. This offers a wide output voltage regulation range but the output voltage is dependent on the load applied to the motor.

In this paper, the closed loop control of PMSM using improved flux weakening controller for traction drive application is simulated and tested. The design of flux weakening controller to overcome the drawbacks and to operate the PMSM in constant power region is discussed in detail. The isolated fly back converter is proposed to avoid the harmonics and to eliminate the disadvantages of the non- isolated converters used in the other system. The simulation model of flux weakening controller, PI controllers, fly back converter and DC to AC converters are also shown.

The goal is to achieve the speed control performance of PMSM with low overshoot, fast response time, low torque and current ripples. The controller is designed to control the speed of the motor in traction applications with load. The design of individual sections are integrated and the performance of the PMSM traction drive is analysed using MATLAB/Simulink toolbox at change of reference speed and motor speed conditions. The accuracy of the field weakening method is discussed with applied load under motor running condition.

2. Design of Field Oriented Control System

In traction drive application, it is necessary to have high speed and torque ranges. To achieve this, in field oriented control, flux weakening method is used in this paper. The flux weakening controller generates reference stator currents which are transformed to d-q axis using the rotation frame theory in park transformation block. These flux and torque producing components are controlled by PI controllers. Figure 1 shows the general structure of field oriented control using flux weakening method.

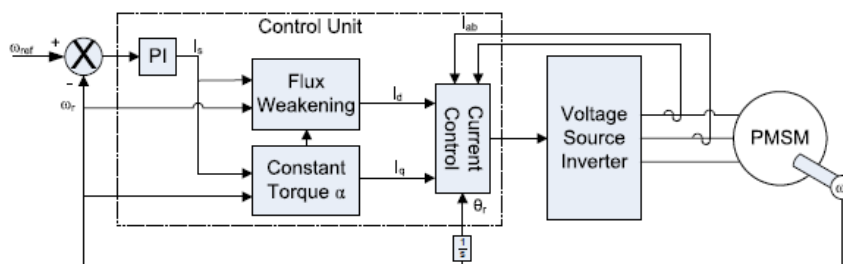


Fig. 1. Typical field oriented control [15].

2.1. Improved flux controller

Maintaining constant speed in traction control system can minimize power loss and improve efficiency of the system to a greater extent. The improved flux weakening control algorithm used in flux controller maintains the speed profile of PMSM. It also eliminates the need of another control unit to determine the switching between constant torque and constant power region. The flux weakening control algorithm switches the motor automatically to different operating regions to provide best performance of the drive. This is achieved by automatic regulation of the direct component of the stator current. To achieve this, the control algorithm continuously samples the instantaneous air-gap magnetic flux and its angle to produce a new direct component of stator current from the rotor position and the speed

The purpose of the controller is to force the actual currents to track the reference currents as fast and as accurate as possible. The dynamics of these current controllers affect the transient and steady state response of the closed loop control system. The flux weakening controller consists of three major blocks that mathematically calculate the reference d-q currents and air-gap flux. The d-q voltage and current equations are shown in Eqs. (1) to (6) [15].

The stator reference currents are calculated as follows:

Rotor position and speed is measured from the motor. The rated speed of the motor is calculated as $N_s = \frac{120f}{P}$ where N_s represents the synchronous speed, f is the frequency and P is the number of the pole of the motors. Reference torque is generated from speed error signal which is regulated by PI controllers in the speed block.

The magnitude and angle of the instantaneous flux is calculated using d-q axis currents according to Eqs. (3) and (4).

$$Vd = Ri_d + p\Phi_d - w_r\Phi_q \tag{1}$$

$$Vq = Ri_q + p\Phi_q + w_r\Phi_d \tag{2}$$

$$\Phi_d = L_d i_d + \Phi_m \tag{3}$$

$$\Phi_q = L_q i_q \tag{4}$$

The electromagnetic torque developed by the machine can be expressed in the d-q axis as shown in Eq. (5).

$$Te = \frac{3}{2} \left(\frac{p}{2} \right) (\Phi_m i_q + p(L_d - L_q) i_q i_d) \tag{5}$$

The q-axis current is calculated from the generated torque using Eq. (6). The non-salient pole PMSM considered whose stator inductances for the d-axis and q-axis are equal, therefore the electromagnetic torque equation reduces to as shown in Eq. (6).

$$Te = \frac{3}{2} \left(\frac{p}{2} \right) (\Phi_m i_q) \tag{6}$$

The d-axis current is calculated from flux magnitude and angle using Eq. (5). PI controllers help to regulate the current errors.

Figure 2 shows the simulation model of field weakening controller using the Eqs. (1) to (6).

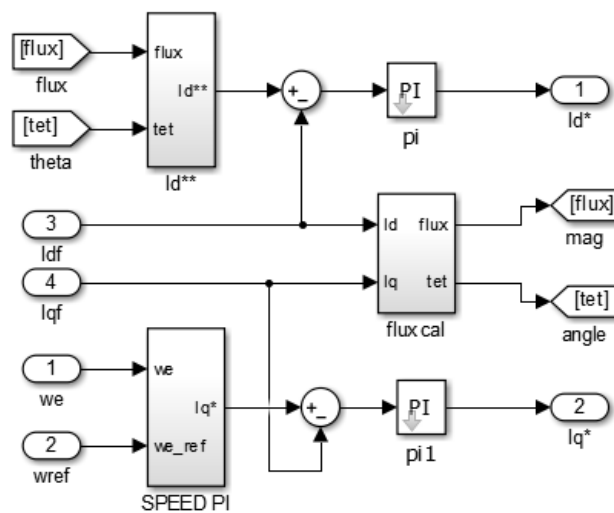


Fig. 2. Flux weakening controller.

The subsystems of d-axis, q-axis and air gap flux calculator blocks shown in Fig. 1 and expanded in Figs. 3 to 5. These blocks are designed using the motor equations.

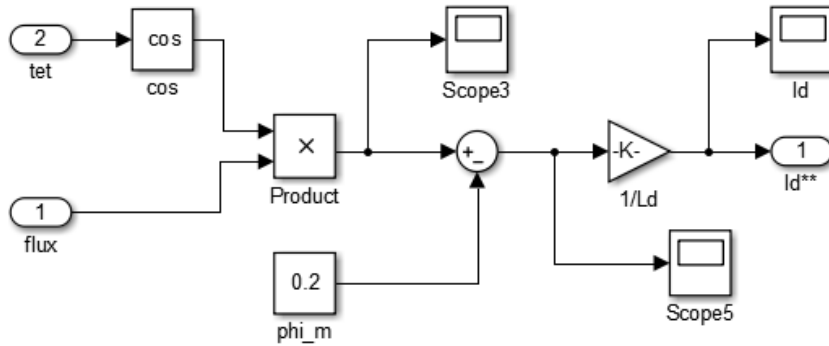


Fig. 3. d-axis reference current calculator.

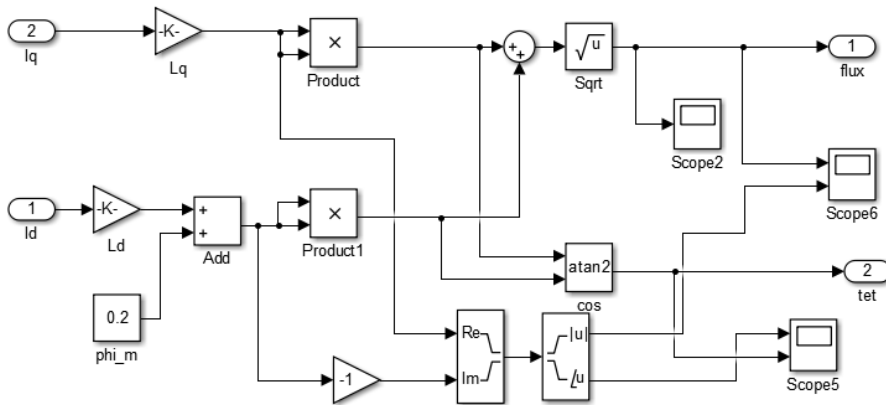


Fig. 4. Air-gap flux calculator.

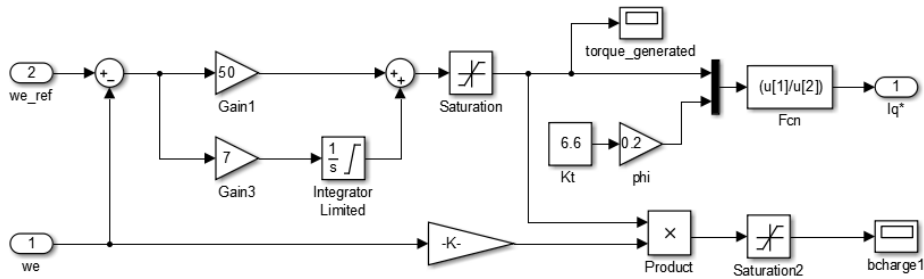


Fig. 5. q-axis reference current calculator.

2.2. Design of DC-DC flyback converter

A high frequency isolated DC-DC fly-back converter is used to provide regulated DC voltage to feed the voltage source inverter. The fly-back converter is a single stage converter in which the voltage error is calculated from the difference between the reference voltage and the actual DC bus voltage at a particular time.

The voltage error is regulated using a PI controller to supply the required current at constant DC bus voltage for any changes in the load or speed. The output of the PI controller is compared to a saw-tooth waveform to generate the switching pulses for the fly-back switch. The initial values of PI controller is chosen using Newton-Raphson method. It continuously changes with output of flyback converter to maintain constant duty cycle. The control algorithm is shown in Fig. 6. The details of flyback converter parameters is given in Appendix A.

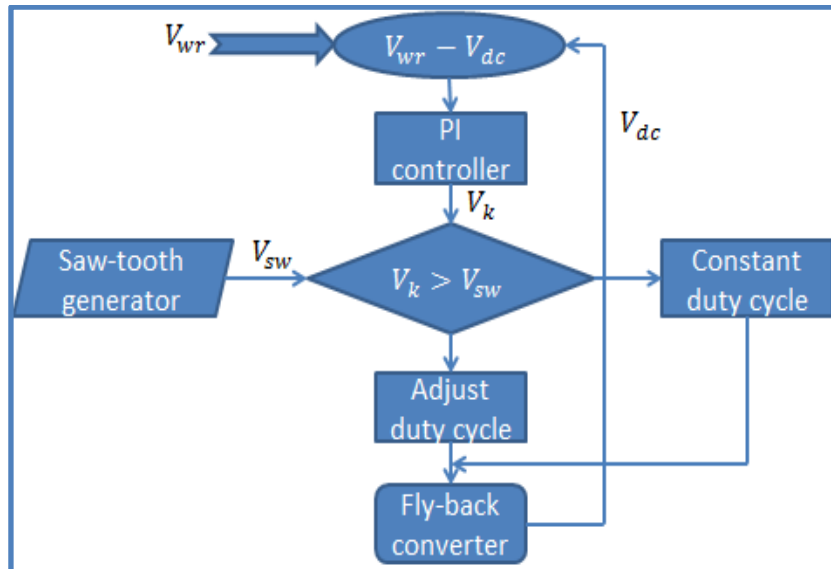


Fig. 6. Control algorithm for fly-back converter.

The PWM current controller sums up the reference and feedback stator currents [16]. The resultant current is compared with the reference saw-tooth wave then the corresponding upper switch in the inverter leg is set high and the lower switch low and vice versa. The simulation model and the switching signal generated are shown in Figs. 7 and 8 respectively.

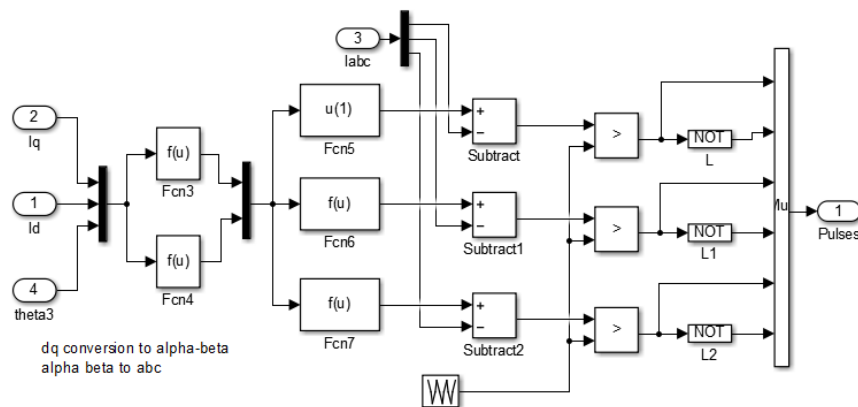


Fig. 7. Current controlled PWM.

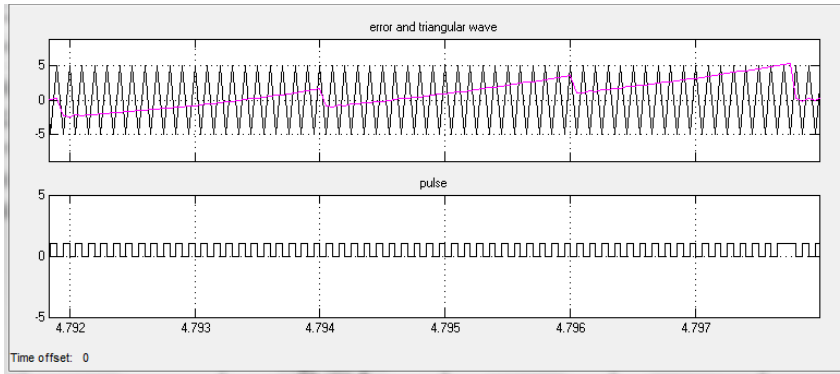


Fig. 8. Pulse generation.

3. Simulation Results and Discussion

The simulation models of the individual sections discussed above are put together to get the complete simulation model shown in Fig. 9. The speed holding capacity of the flux weakening control of PMSM drive at different operating conditions. The X-value of the graphs is measured in time in sec and Y-value of the graphs is measured in Nm and rad/sec for torque and speed respectively. The motor parameters are given *Appendix B*.

To supply large amount of energy for an extended period of time a battery is used to feed the traction model. A three phase voltage source inverter with six IGBTs is used as the power electronic interface between the fly-back converter and PMSM motor. The six IGBTs control the input currents of PMSM. A second order low pass filter is used to reduce the current ripples and this increases the overall efficiency of the traction system. A protection scheme to prevent the abnormal voltages on DC bus during braking mode of the motor is also included in the system

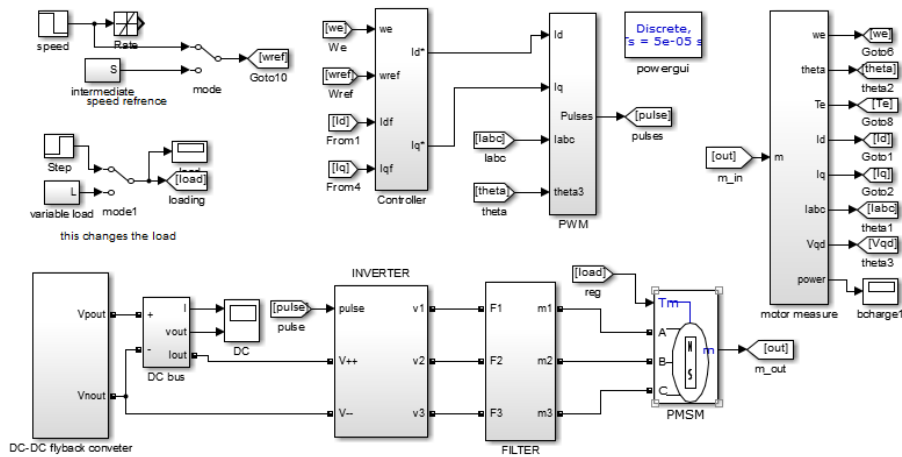


Fig. 9. Simulation model of the complete system.

The integrated system is tested under three mode of operation of the PMSM motor. In all simulations the motor is assumed to have an initial mechanical load torque connected and in practical cases this can be considered as weight of the complete drive. The speed, torque, stator currents, stator voltage results for load variations are presented.

3.1. Running mode

The reference speed of the motor is set to 500 rad/s and different mechanical load torques are applied and removed at different times as shown in Fig. 10. It can be seen from Fig. 11 that the speed of the motor is maintained constant for the changes in load torque.

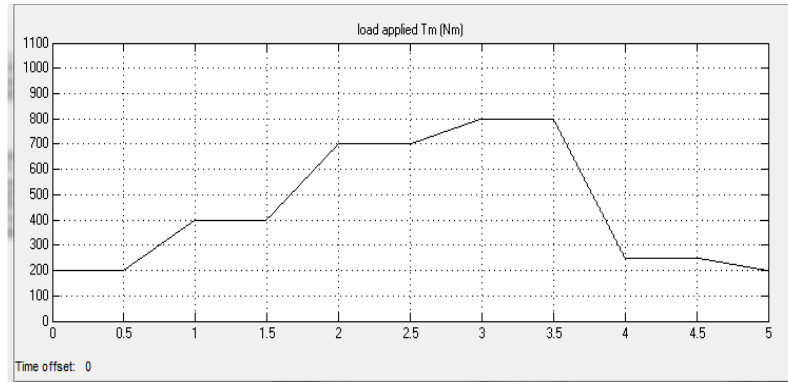


Fig. 10. Load torque applied at a speed of 500 rad/s.

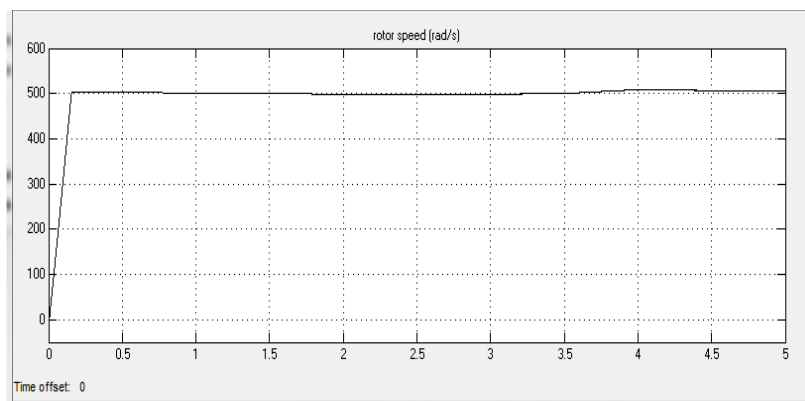


Fig. 11. Rotor speed response at different load torque.

Though the speed of the motor is maintained constant small dips can be observed on the speed profile during loading. It shows that during the loading, the desired speed is delivered with 2.6% of ripple for mechanical load torque ranging from 200 Nm to 800 Nm as shown in Fig. 12. This shows that the speed difference between the desired speed and speed of the rotor was quickly compensated by the field weakening controller. Also the speed is regulated within

the acceptable ranges during the loading period due to good dynamic performance of the field weakening controller.

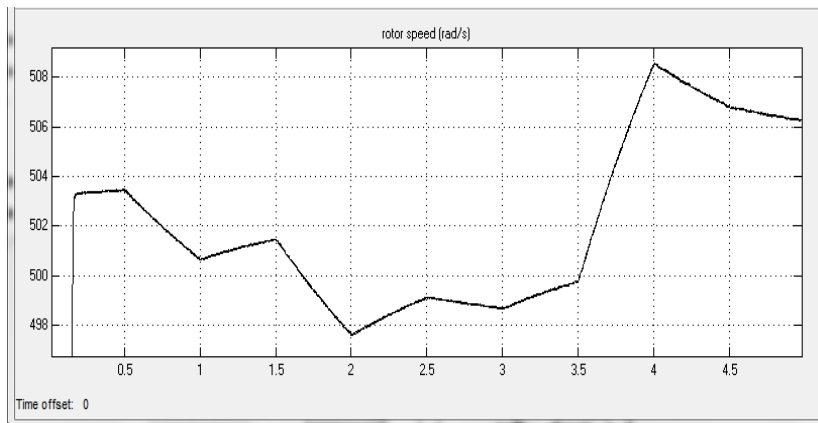


Fig. 12. Rotor speed changes (zoomed).

The effect of changes in load torque due to changes in stator current is shown in Fig. 13. It can be seen that the stator current increases at the moment the load torque is applied while the frequency of the stator currents is maintained constant. The frequency does not change because the speed of the PMSM is maintained constant during the torque changes. As the load torque increases, to meet the high starting torque of the PMSM motor, the quadrature component of stator current is increased to generate more accelerating torque. The corresponding developed torque is shown in Fig. 14. It can be seen that the transitions of the developed torque are similar to mechanical load torque except at starting where more torque is needed to overcome the weight and frictional forces of the system.

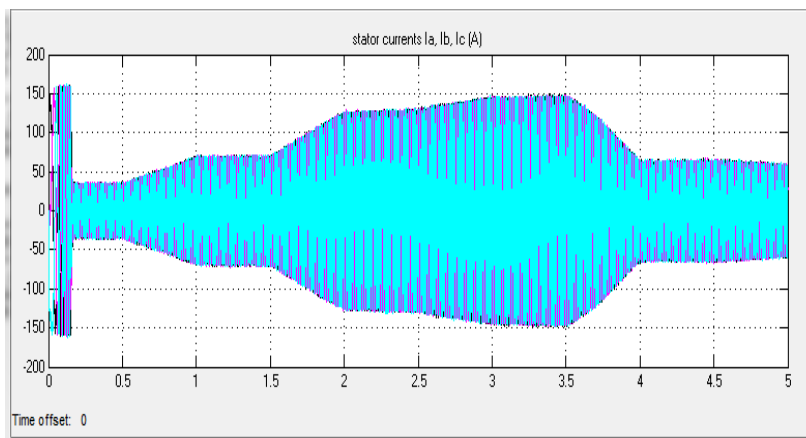


Fig. 13. Stator currents during motor loading.

During the motoring mode, the direct component of stator current is expected to be always below zero and the quadrature component above zero. According to the decoupling principle of the field oriented control, the quadrature component must be above zero to generate positive torque and changes linearly with the torque needed. This can be seen from Figs. 15 and 16. The DC bus current and voltage

during loading is shown in Fig. 17. It can be seen to reduce the speed error and to maintain the optimal performance of the motor, the DC bus voltage is maintained constant at 560 V and the current is maintained similar to the stator currents.

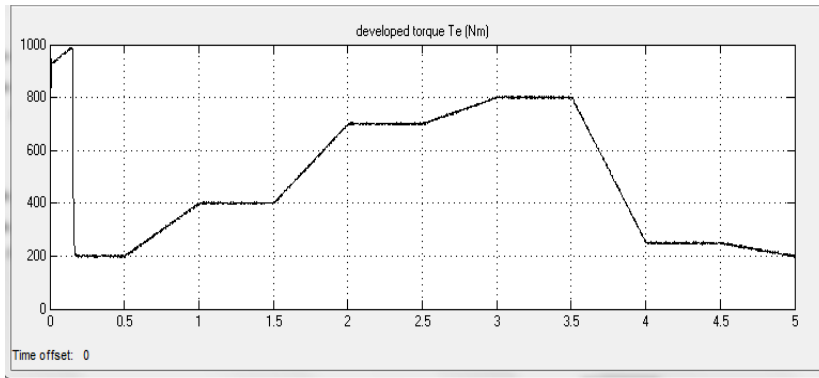


Fig. 14. Developed torque.

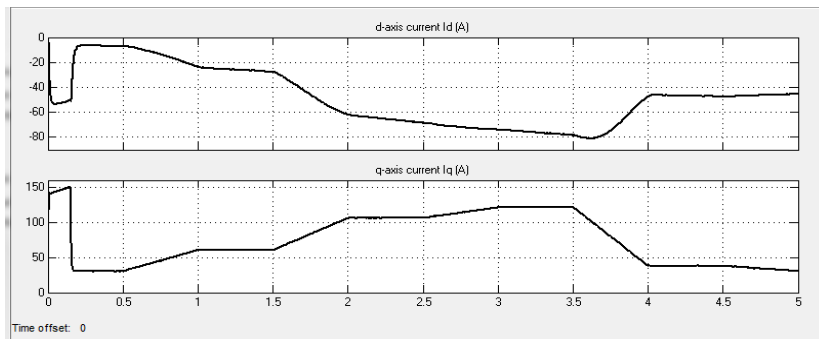


Fig. 15. d-q stator currents.

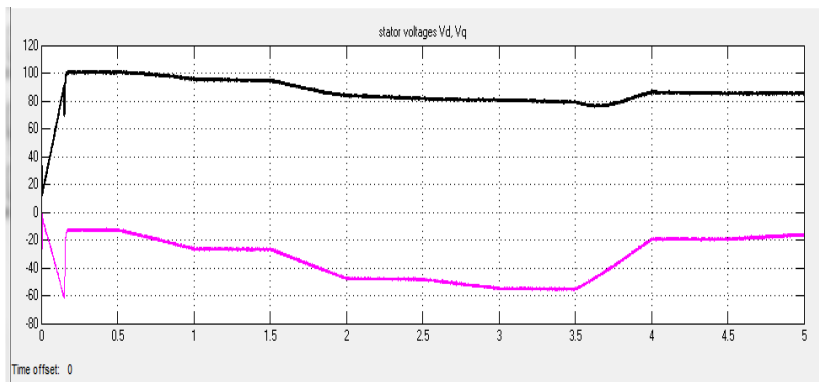


Fig. 16. d-q stator voltages.

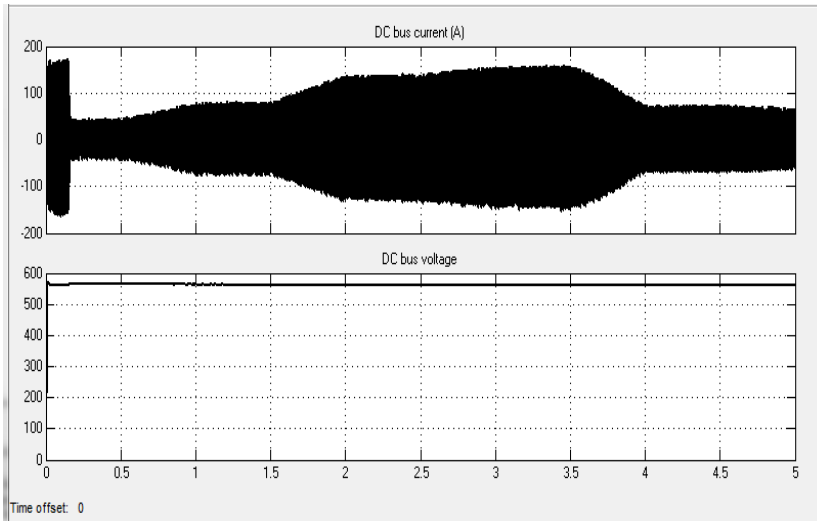


Fig. 17. DC bus voltage and current.

3.2. CASE 2: Inter-mediate stop mode

In this mode a drive cycle was implemented to accelerate the motor from rest and decelerate it at different intervals. The time to bring the motor to rest can be increased by changing the gradients of transitions in a look-up table. The motor drive cycle to illustrate the inter-mediate stop operation is shown in Fig. 18.

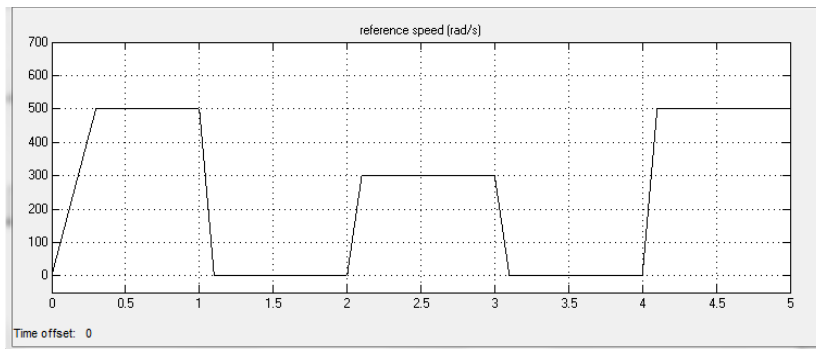


Fig. 18. Motor drive cycle.

The developed torque and the motor speed for the change in speed is shown in Figs. 19 and 20 respectively. It can be seen that during the deceleration of the motor, a negative torque signal is passed to the field weakening controller to bring the motor to rest. This causes the motor to operate in the second quadrant region. It can also be seen from Fig. 20, the motor speed follows the reference speed with good accuracy, minimum speed overshoot and ripples.

The change in stator currents for changes in reference speed is shown Fig. 21. It can be seen that during acceleration time, current is limited to the maximum value and this gives maximum acceleration torque according to the torque equation. However, during the steady state, the currents are reduced to produce

torque to overcome the mechanical load torque. During deceleration, the current stays at the same magnitude as in steady state condition at low frequency. The stator current is not reduced to zero to illustrate the situation where the motor is on a climb-hill and braking mode is applied. Under this situation, it is required to stop the motor without backward movement.

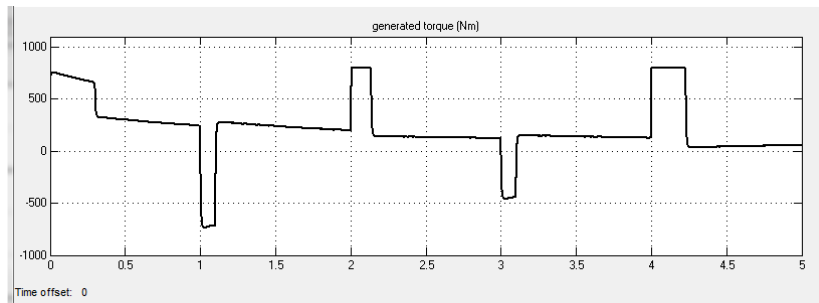


Fig. 19. Generated torque.

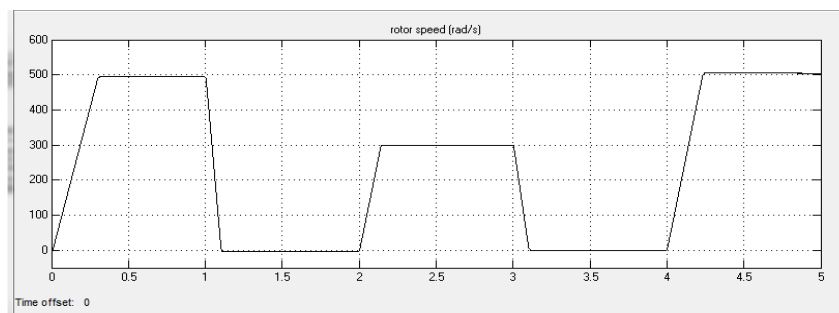


Fig. 20. Rotor speed.

To meet this condition, the motor has to produce some torque to overcome the total load of the system and in this illustrated in Fig. 19, with the load not removed during the deceleration of the motor to rest. Hence the stator current is not reduced to zero as shown in Fig. 21.

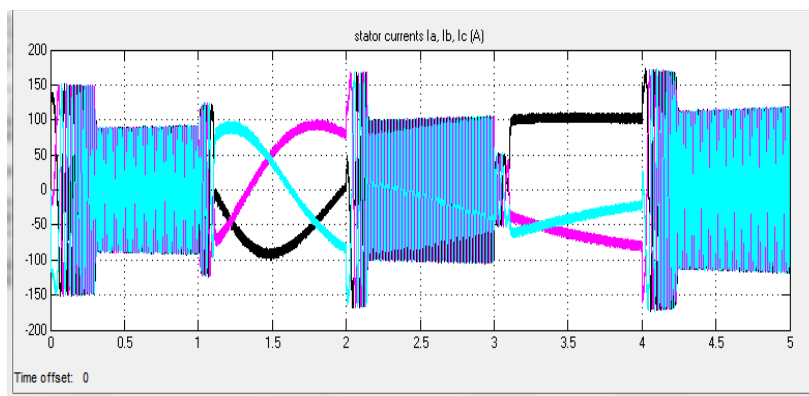


Fig. 21. Stator currents.

In running mode, the load torque is changed from 200 Nm to 800 Nm and motor speed is maintained at 500 rad/s. In Intermediate Stop mode, the load torque is changed from 480 Nm, 100 Nm and 50 Nm. It can be seen from fig. 20 that the motor speed tracks the reference speed irrespective of the torque changes. Also the motor current is maintained around 100A in all torque conditions. From the speed and torque graphs it can be seen that the field weakening algorithm drives the motor into the flux weakening region with good speed and torque dynamics.

4. Conclusion

Permanent magnet synchronous motors (PMSMs) provide a competitive technology for EV traction drives owing to their high power density and high efficiency [17]. It is essential to drive the motor at constant speed in most of the traction applications to minimize the power loss and improve efficiency. In this research, PMSM using field weakening control method is developed and tested to suit the different operations of traction applications. The PMSM is chosen in this application because it is difficult for DC motors to achieve speeds above its base speed in traction applications. Induction motors can reach the speeds with increased slip but at the expense of efficiency and complexity of the traction system.

Using the proposed flux weakening control method for PMSM in traction drive applications, it can be noted that the actual speed of the tracks the reference speed accurately in all modes of operation. Also, from the shape of the developed torque and quadrature component of the stator current it can be seen that the PMSM can be controlled easily like a DC motor using flux weakening control technique. It is observed that from the onset of the direct component of the stator current below zero at very low speeds, the motor can go as far as 800 rad/s. The overshoots and ripples were kept low using the flux weakening control.

However disadvantage of the proposed field weakening control is, it is relatively slow and produces overshoots in actual values at set points when step commands are used. This was solved by using ramp signals in simulation. However, developed torque curves are steeper and in real practice this can cause wheel slip during starting of the motor. This can be improved by implementing neural network based controller to compensate the flux and torque according to changes in speed.

References

1. Puranen, L. (2006). *Induction motor versus permanent magnet synchronous motor in motion control Applications: a comparative study*. PhD Dissertation, Lappeenranta University of Technology, Finland, 30-35.
2. Vindel, D.; Haghbin, S.; Rabiei, A.; Carlson, O.; and Ghorbani, R. (2012). Field oriented control of a PMSM using the dSPACE controller. *IEEE International Conference on Electrical Vehicles*, 1-5.
3. Simank, J.; Novák, J.; Doleček, R.; and Černý, O. (2007). Control algorithms for permanent magnet synchronous traction motor. *The International Conference on "Computer as a Tool" EUROCON*, 1839-1844.

4. Zhang, J. (2008). *Bi-directional DC-DC power converter, design optimization, modeling and control*. Ph.D. dissertation, Virginia Polytechnic Institute and State University.
5. Huang, X.-Y.; Zhang, J.-C.; Sun, C.-M.; Huang, Z.-W; Lu, Q.-F.; Fang, Y.-T.; and Yao, L. (2015). A combined simulation of high speed train permanent magnet traction system using dynamic reluctance mesh model and Simulink. *Journal of Zhejiang University-Science*, 16(6), 607-615.
6. Sun, T.; Wang, J., and Chen, X. (2015). Maximum torque per ampere (MTPA) control for interior permanent magnet synchronous machine drives based on virtual signal injection. *IEEE Transactions on Power Electronics*, 30(9), 5036-5045.
7. Shakilabanu, A.; and Wahidabanu, R.S.D. (2013). BELBIC based high performance IPMSM drive for traction. *Journal of Theoretical and Applied Information Technology*, 57(3), 631-639.
8. Kassem, A.M.; and Hassan, A.A. (2012). Performance improvements of a permanent magnet synchronous machine via functional model predictive control. *Journal of Control Science and Engineering*, Article ID 319708, 8 pages.
9. El Shahat, E.; and El Shewy, E. (2010). Permanent magnet synchronous motor drive system for mechatronics applications. *International Journal of Research and Applied Sciences*, 4(3), 324-325.
10. Kondo, M. (2003). Application of permanent magnet synchronous motor to driving railway vehicles. *Railway Technology Avalanche*, 1, page 6.
11. Doleček, R.; Novák, J.; and Černý, O. (2009). Traction permanent magnet synchronous motor torque control with flux weakening. *Radioengineering*, 18(4), 601-605.
12. Agarwal, J.P. (2001). *Power electronics systems: Theory and design*. Prentice Hall.
13. Iker Kayaalp, R.; Demirdelen, T., Mehmet, T. (2015). Modelling and analysis of bidirectional DC-DC converter. *International Journal for Innovation Education and Research*, 3(12), 16-30.
14. Jil, S.; Manisha, S.; and Chirag, C. (2013) . Comparative analysis of single phase and multiphase bidirectional DC-DC converter. *International Journal of Emerging Trends in Electrical and Electronics*, 2(1), 41-46.
15. Bose, B.K. (2002). *Modern power electronics and AC drives*. Prentice Hall.
16. Sreeharsha, C.; Das, A.; and Pradabane, S. (2009). Study of sinusoidal and space vector pulse width modulation techniques for a cascaded three-level inverter. *International Journal of Research in Engineering and Technology*, 2(9), 365-370.
17. Zhang, Y.; Cao, W.; McLoone, S.; and Morrow, J. (2016). Design and flux weakening control of an interior permanent magnet synchronous motor for electric vehicles. *IEEE Transactions on Applied Superconductivity*, 26(7).

Appendix A**Traction drives specifications**

Battery supply voltage 300 V
 Maximum operating current 200 A
 Maximum output power of fly-back converter 60 kW
 Fly-back converter switching frequency 50 kHz
 DC bus voltage 560 V
 Drive switching frequency 10 kHz
 Transformer turns ratio 2

Appendix B**PMSM motor Specifications**

Parameter	symbol	Value
Rated torque	T_r	1100 Nm
Rated speed	N_r	5000 rpm
Stator resistance	R_s	0.0085 Ω
Stator Inductance	L_q, L_d	0.0008 H
Flux constant	Φ_m	0.2
Moment of inertia	J	0.011 kg/m ²
Viscous coefficient	B	0.001889
Pole pairs	p	22